THE JOURNAL OF PHYSICAL CHEMISTRY Letters

pubs.acs.org/JPCL

Letter

Quantum Control of Ultrafast Internal Conversion Using Nanoconfined Virtual Photons

Aleksandr G. Avramenko and Aaron S. Rury*

Cite This: *J. Phys. Chem. Lett.* 2020, 11, 1013−1021

Read Online

ACCESS | Metrics & More | Article Recommendations | Supporting Information

ABSTRACT: The rational control of nonradiative relaxation remains an unfulfilled goal of synthetic chemistry. In this study, we show how strongly coupling an ensemble of molecules to the virtual photons of an electromagnetic cavity provides a rational handle over ultrafast, nonradiative dynamics. Specifically, we control the concentration of zinc tetraphenyl porphyrin molecules within nanoscale Fabry−Perot cavity structures to show a variable collective vacuum Rabi splitting between cavity polaritons coincides with systematic changes in internal conversion rates. We find these changes deviate from the predictions of so-called gap laws. We also show that simple theories of structural changes caused by polariton formation cannot explain discrepancies between our results and established theoretical predictions. In light of these deficiencies, we explore other ways to explain the dependence of the internal conversion rate on polariton parameters. Our results demonstrate cavity polariton formation controls the photophysics of light harvesting and photocatalytic molecular moieties and the gap remaining in our fundamental understanding of mechanisms enabling this control.

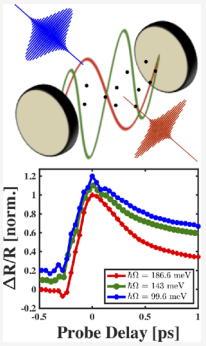

Relaxation is the most important step in determining the utility of a light-absorbing or -emitting substance. The presence of insufficient nonradiative relaxation from a highly absorbing electronic state to a lower-lying state more capable of forming a desired chemical product or emitting a useful photon can inhibit the applicability of specific molecules and materials for next-generation photochemical and optoelectronic platforms. Given this reality, the ability to control nonradiative relaxation mechanisms remains a potentially transformative goal.

Despite the need to control nonradiative relaxation, especially on ultrafast time scales, traditional chemical methods using solution or solid phase synthesis remain incapable of controlling these processes deterministically. In specific cases of metal-centered complexes designed for photocatalytic and optoelectronic technologies, studies show the rate of nonradiative relaxation can be controlled by modulating the energy gap between participating electronic states.[1−3] What remains unclear, however, are hard and fast rules quantitatively connecting synthetic principles, such as the Hammett parameter, with changes to these energy gaps. Because we lack the ability to predict relationships between the structures and dynamics of specifically targeted molecules accurately, these connections do not exist. Furthermore, even with the clarification of these connections, it is not clear that synthetic methods have been developed to produce such molecular targets in sufficiently high yields. In the absence of traditional synthetic methods to control the flow of energy between molecular states with deterministic precision, we seek alternative strategies to manipulate ultrafast relaxation dynamics central to potentially transformative advances in photocatalytic and optoelectronic applications.

The strong coupling of light to material electrons leads to the formation of hybrid light-matter states known as polaritons. When one embeds molecules into a sufficiently high quality electromagnetic resonator, the molecular electrons can strongly couple to quantum mechanically fluctuating, virtual photons within the resonator's shaped photonic density of states. When strong coupling occurs within such a resonator, cavity polaritons form, and their energies separate by a gap proportional to the coupling strength known as the vacuum Rabi splitting energy, $\hbar\Omega$.[4] Despite being first demonstrated more than 20 years ago,[5] the effects of cavity polariton formation on the ultrafast relaxation processes of complex molecules central to their potency in photocatalytic and optoelectronic applications remain unclear.

For example, the large transition dipole moment of the Soret transition of metalloporphyrins has made these systems ideal choices for light harvesting,[6−8] electron and energy transfer,[9] and artificial photosynthesis,[10−12] whose primary physical processes include nonradiative relaxation on ultrafast time scales. However, an incomplete understanding of how polariton formation in nanoscale cavities affects these ultrafast relaxation processes inhibits the rational design of resonator structures to control photophysical and photochemical processes of this well-established class of molecules using quantized virtual photons. Most importantly, whether cavity polariton formation changes the electronic and nuclear

Received: November 21, 2019
Accepted: January 17, 2020
Published: January 17, 2020

https://dx.doi.org/10.1021/acs.jpclett.9b03447
J. Phys. Chem. Lett. 2020, 11, 1013−1021

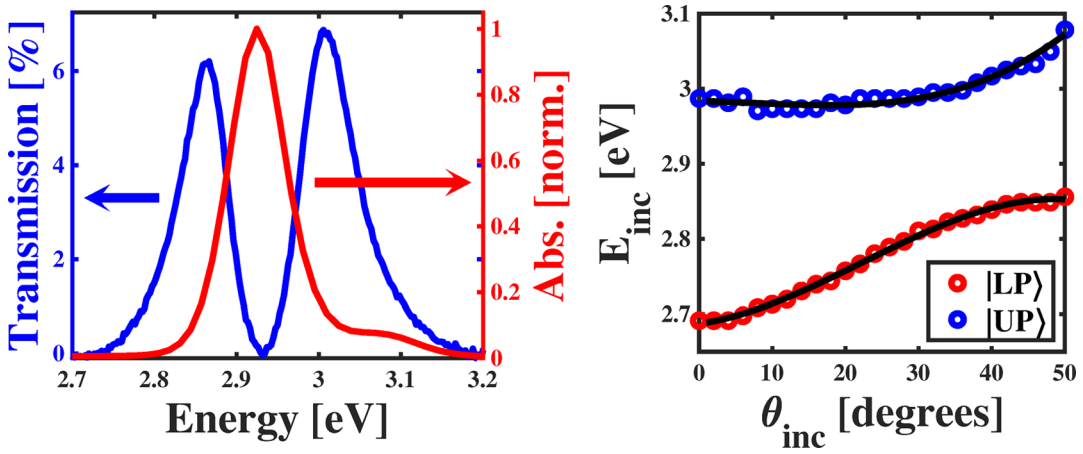

Figure 1. Comparison of the linear ultraviolet−visible absorption spectrum of a PMMA film doped with ZnTPP in the region of the molecule's Soret resonance (red) to the transmission spectrum of the Fabry−Perot cavity structure described in the text at an incident angle of 44° (blue) possessing a collective vacuum Rabi splitting energy of ∼186.6 meV (left). Comparison of the dispersion of the energy of the lower polariton (|LP⟩) to that of upper polariton (|UP⟩) observed by changing the angle an incident beam makes with the direction normal to the surface of the cavity structure (right).

structure of strongly coupled molecules central to their photochemical reactivity, as predicted by theory, remains unclear.[13−18] In this study, we demonstrate cavity polariton formation can be used to deterministically control ultrafast internal conversion rates between the excited singlet states of zinc(II) tetraphenyl porphyrin (ZnTPP), a model system for light harvesting, and energy transfer moieties. Moreover, these results do not conform with the canonical theory of nonradiative relaxation.

The collective coupling of the quantum mechanically fluctuating virtual photons of an electromagnetic resonator to cavity-embedded molecules provides a powerful handle over the vacuum Rabi splitting energy between the cavity polariton states.[4] Specifically, as one loads more molecules into the cavity structure, one can increase the vacuum Rabi splitting by a known amount for a given cavity length.[5] For the case of ZnTPP, this increasing vacuum Rabi splitting will drive the energy of the lower polariton closer to that of the first excited singlet state, S_1. As we show below, this collective, quantum mechanical control over the energy gap between polaritonic and nonpolaritonic states translates directly into control over the rate of ultrafast relaxation between them.

The left panel of Figure 1 compares the linear absorption spectrum of an ∼200 nm poly(methyl methacrylate) (PMMA) film doped with ZnTPP to the transmission spectrum of a Fabry−Perot cavity structure containing an ∼140 nm ZnTPP-doped PMMA film embedded within it. The cavity structure was fabricated as described in Methods. For the case of Figure 1, the incident beam makes an angle of 44° with respect to the cavity structure's surface normal. Unlike the single, prominent Soret peak and small blue-shifted shoulder of the linear absorption spectrum of the free space film, Figure 1 shows the cavity transmission spectrum possesses two peaks corresponding to the upper and lower polaritons. The slightly higher intensity of the upper polariton peak suggests we detuned the cavity to the blue side of the Soret resonance of ZnTPP at this incident angle. The slight asymmetry of the line shape of the upper polariton peak results from losses in the Al layer used to cap the Fabry−Perot structure, as seen in Figure S1.

The right panel of Figure 1 shows the avoided crossing in the dispersion of the loaded cavity structure as we tune through different incident angles. At the angle shown in the left panel of Figure 1, we find the vacuum Rabi splitting energy between the polaritons is 186.6 meV. Figure S2 shows as we decrease the concentration of the ZnTPP in each cavity structure, the vacuum Rabi splitting also decreases. As shown in Figure S2, at a film concentration near 15 mM, we can still resolve distinct cavity polariton peaks separated by a vacuum Rabi splitting of 99.6 meV.

To assess the ability of cavity polariton formation to control the ultrafast relaxation dynamics of strongly coupled ZnTPP molecules, we undertook measurements of the ultrafast dynamics of solution phase molecules and cavity polariton samples. We pumped both types of samples at 3.10 eV (400 nm) and compared their dynamical response at 1.970 ± 0.015 eV (630 ± 10 nm). Zewail and co-workers observed a transient absorption signal in this spectral window whose initial decay matches that of the internal conversion from the S_2 state to the S_1 state in solution phase ZnTPP molecules, as established from their time-resolved photoluminescence measurements following 3.12 eV (397 nm) excitation.[19] In the case of our cavity polariton measurements, the 3.1 eV pump pulse either directly excites the upper polariton for the largest values of the vacuum Rabi splitting energy we examine or excites the sample just above the upper polariton. Given previous studies, we expect excitation above the upper polariton should engage the polariton dynamics.[20,21] However, by probing an excited state absorption process off resonance with polaritonic transitions, we are not sensitive to intrapolariton relaxation processes and can instead focus our attention on how polariton formation affects ultrafast conversion into nonpolaritonic states. This approach contrasts with previous studies. Lidzey and co-workers examined the angle-resolved dynamics of ZnTPP in similar cavity polariton samples previously,[22] but they pumped and probed the lower polariton only for a single vacuum Rabi splitting value and did not compare their results directly to those from solution phase measurements.

Figure 2 shows the ultrafast transient reflectivity of ZnTPP cavity polaritons probed at 1.97 eV following excitation at 3.1 eV. The data in Figure 2 suggest the ultrafast transient reflectivity of these cavity polaritons depends on not only polariton formation but also the strength of the coupling

https://dx.doi.org/10.1021/acs.jpclett.9b03447
J. Phys. Chem. Lett. 2020, 11, 1013−1021

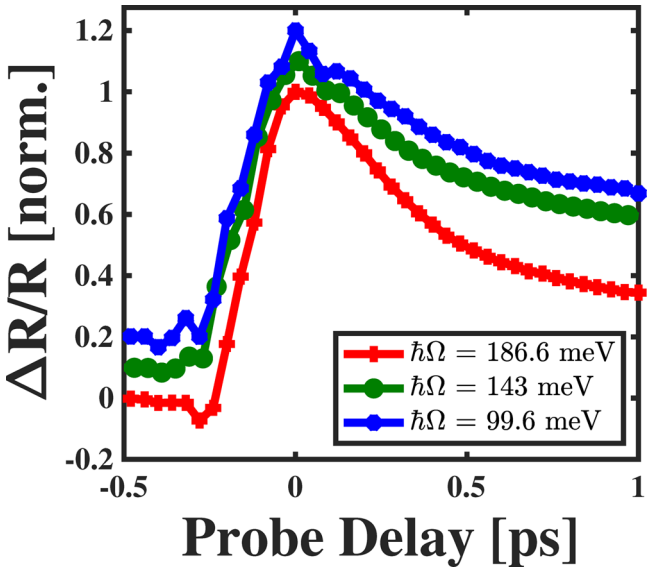

Figure 2. Comparison of the ultrafast transient reflectivity of the 1.970 ± 0.015 eV band of a white light continuum probe pulse from zinc(II) tetraphenyl porphyrin cavity polariton samples following 3.1 eV excitation for collective vacuum Rabi splitting energies of 186.6 meV (red), 143 meV (green), and 99.6 meV (blue) for the probe delay window between −0.5 and 1 ps. The kinetic traces have been offset vertically to more easily compare them visually.

between the molecules' Soret resonance and the cavity's virtual photons. Specifically, Figure 2 suggests that as we increase the collective vacuum Rabi splitting by concentrating more ZnTPP in the cavity, the initial relaxation rate of the associated kinetic trace increases. The transient absorption we measure for solution phase ZnTPP molecules is shown in Figure S3. To more firmly establish a quantitative trend between the ultrafast internal conversion rate and the collective vacuum Rabi splitting of the cavity polaritons, we fit their transient reflectivity kinetic traces, $S(t)$, to the following function:

$$S(t) = A_1 e^{-k_1 t} + A_2 e^{-k_2 t} + A_3 e^{-k_3 t} \cos(\omega_{ph}\{t - t_0\}) \quad (1)$$

where A_1 is the amplitude of the contribution to the signal we attribute to ZnTPP and k_1 is its decay rate. Given the work of Zewail, we assign the first contribution to eq 1 as the internal conversion between the delocalized, lower-cavity polariton and the S_1 state of individual ZnTPP molecules. Given the 2 ns lifetime of the S_1 state as established previously, we assign A_2 and k_2 in eq 1 as the amplitude and decay rate, respectively, of the photoexcitation in the Al film used to cap the Fabry−Perot structure. In addition, we assign the terms A_3, k_3, ω_{ph}, and t_0 in eq 1 as the amplitude, decay rate, angular frequency, and time delay of an acoustic phonon our pump pulse coherently launches in the Al layer, respectively, as has been demonstrated in many metallic nanomaterials.[23−26] To fit the kinetic traces to eq 1, we first deconvolute a Gaussian possessing a temporal

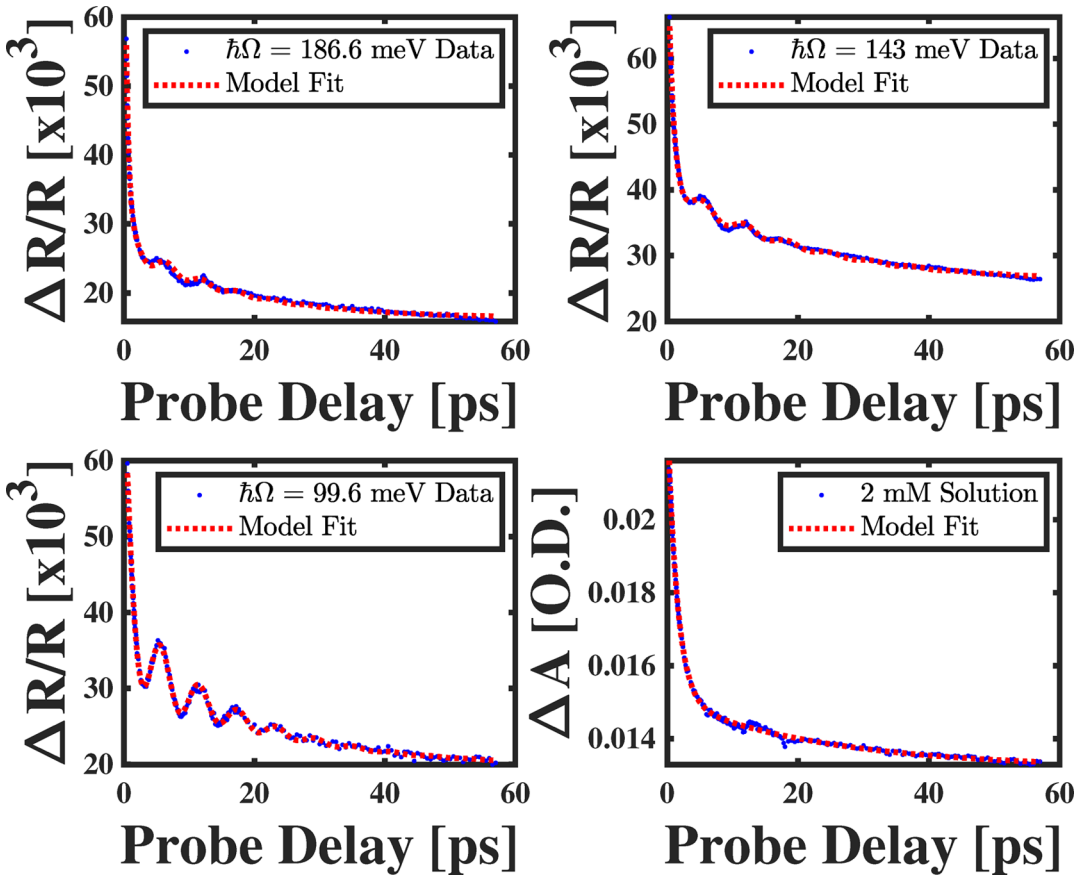

Figure 3. Comparison of the experimentally measured and theoretically modeled ultrafast transient dynamics of ZnTPP in Fabry−Perot cavity structures possessing collective vacuum Rabi splitting energies of 186.6 meV (top left), 143 meV (top right), and 99.6 meV (bottom left). In addition, the bottom right panel shows our analysis of the solution phase ultrafast transient absorption of a 2 mM solution of ZnTPP dissolved in toluene.

https://dx.doi.org/10.1021/acs.jpclett.9b03447
J. Phys. Chem. Lett. 2020, 11, 1013−1021

full width half-maximum of 147.1 fs, as determined by comparison to the initial rise of the transient reflectivity signal. This Gaussian contribution results from the nonlinear response of the sample due to the temporal overlap of the pump and probe pulses. The values for all of the parameters extracted from fitting the measured kinetic trace to eq 1 for each ZnTPP sample are reported in Table S1.

The panels of Figure 3 compare the kinetic traces of the ultrafast transient reflectivity dynamics of four separate ZnTPP samples and nonlinear regression fits to two separate physical models. For three of these panels, we compare the measured dynamics of cavity polaritons formed from different concentrations of ZnTPP molecules within Fabry−Perot cavity structures to the results of fitting the data to eq 1. In the bottom right panel of Figure 3, we compare the ultrafast transient absorption signal of ZnTPP molecules dissolved in toluene to a simple physical model containing only the first two terms of eq 1, as described in the Supporting Information.

By inspecting these comparisons carefully, we reach three important conclusions. First, the oscillations of the acoustic phonon launched in the Al layer of each cavity structure become more prominent as we reduce the collective vacuum Rabi splitting. This effect results from the reduced overlap of the pump pulse with the upper polariton state as we reduce the vacuum Rabi splitting energy. As this overlap decreases, so does the size of the signal stemming from the cavity-embedded ZnTPP molecules relative to that of the coherent acoustic phonon. As such, the signal from the coherent acoustic phonon appears to be more prominent as we reduce the vacuum Rabi splitting. Second, there are small differences in the signal at long probe delays for the different cavity structures. We believe this effect arises from differences in the reflectivity change of the Al layers. As one can see in Table S1, we find the cavity structure possessing a collective vacuum Rabi splitting energy of 143.0 meV also possesses the lowest coherent acoustic phonon frequency of the three cavity samples. Given this frequency depends on the material speed of sound, ν, and layer thickness, L, according to the relation $\omega_{ph} = \pi\nu/L$, we can conclude this cavity structure also possesses the thickest Al layer, which allows it to absorb the most pump photons. Because this layer absorbs the most photons, we expect the transient reflectivity signal from this structure to be larger than those of the other cavity structures investigated in our study. Third, the sufficient agreement between the measured data and the physical models shows we can use eq 1 as a basis to understand how the differences in the dynamics of the ZnTPP molecules depend on the quantum mechanically fluctuating electromagnetic environments in which we embed them.

The dependence of the internal conversion decay rate on the collective vacuum Rabi splitting energies found from our fitting analysis is reported in Table 1. In addition, Figure 4 shows the results of this analysis schematically. In particular, we find that as we increase the collective vacuum Rabi splitting and bring the lower polariton state closer in energy to the S_1 state, the internal conversion rate increases. This result indicates we can control the rate of nonradiative relaxation between different excited states of the light-matter system through changes in the molecular concentration within the cavity. These changes also seem to be independent of the relaxation process into the lower polariton from the upper polariton we excite initially with our 3.1 eV pump pulse. Lidzey and co-workers show the intrapolariton relaxation should occur at rates significantly higher than those we find in this analysis.[27] This significant difference suggests we do not probe the intrapolariton relaxation process as expected from our experimental design.

Table 1. Comparison of the Initial Decay Rate Constants Found by Modeling the Ultrafast Transient Reflectivity Dynamics of Cavity Polaritons Formed from Zinc(II) Tetraphenyl Porphyrin (ZnTPP) Probed at 1.970 ± 0.015 eV following a 3.1 eV Pump Pulse Using eq 1 for Three Different Collective Vacuum Rabi Splitting Values

$\hbar\Omega$ (meV)	k_1 (ps^{-1})
0[a]	0.67 ± 0.02
0[b]	0.67 ± 0.09
99.6	0.87 ± 0.07
143.0	1.28 ± 0.07
186.6	2.25 ± 0.10

[a]These values are compared to solution phase kinetics of ZnTPP dissolved in toluene measured for this study. [b]These values are compared results from a similar experiment reported by Zewail and co-workers in ref 19.

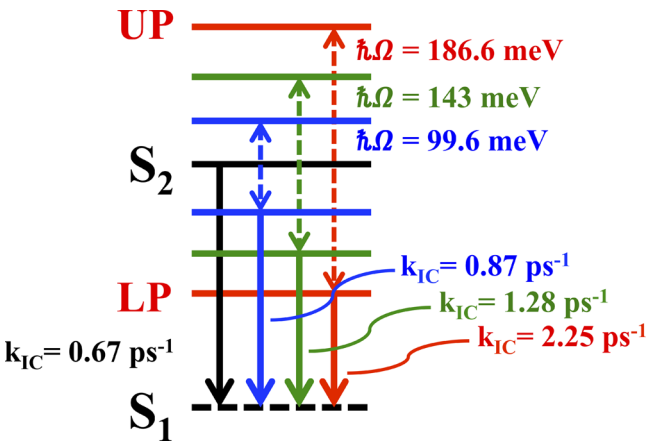

Figure 4. Schematic representation of the change in the ultrafast internal conversion decay rate, k_{IC}, as a function of the value of the collective vacuum Rabi splitting between the energies of cavity polaritons formed using the Soret transition of zinc(II) tetraphenyl porphyrin (ZnTPP) molecules. As we reduce the energy gap between the S_2 and S_1 states of solution phase ZnTPP molecules (black) with polaritons separated by 99.6 meV (blue), 143 meV (green), and 186.6 meV (red), k_{IC} increases to the color-coded values reported in the schematic.

With the trends in the ultrafast internal conversion rate between polaritonic and nonpolaritonic states established rigorously above, we seek a microscopic physical model capable of describing how the properties of photoexcited molecules change upon polariton formation. Several authors developed theoretical descriptions of the dominant determinants of nonradiative relaxation between the electronic states of large molecules.[28−33] In particular, Jortner and several co-authors developed theories explaining the rate of nonradiative relaxation between the excited electronic states of aromatic molecules, like metalloporphyrins.[31−33] In their most prominent theory, these authors proposed the nonradiative rate obeys a relationship that depends on the energy gap between involved states, written as

$$k_{IC} = \frac{C^2\sqrt{\pi}}{\hbar\sqrt{\hbar\omega_\nu \Delta E}} \exp\left\{-\Delta E/\hbar\omega_\nu\left[\log\left(\frac{2\Delta E}{\hbar\omega_\nu \Delta_\nu^{\,2}}\right) - 1\right]\right\} \quad (2)$$

https://dx.doi.org/10.1021/acs.jpclett.9b03447
J. Phys. Chem. Lett. 2020, 11, 1013−1021

where C is the nonadiabatic coupling between the electronic states due to the nuclear kinetic energy operator, ω_ν is the frequency of a vibration involved in the nonradiative transition, Δ_ν is the dimensionless displacement between the two involved states along that vibration, and ΔE is the energy gap between the ground vibrational states of each respective electronic manifold.

In addition to its direct dependence on ΔE, eq 2 suggests the decay rate of internal conversion stems from two separate but related nuclear structural effects. First, because internal conversion must occur via the excited vibrational states of the lower-lying electronic manifold, the overlaps of the vibrational states, known as Franck−Condon factors, between the different manifolds also control the decay rate. In the case of large structural differences between the involved electronic states, significant Franck−Condon factors exist between the lowest-lying vibrational state of the relaxing electronic manifold and highly excited vibrational states of its electronic counterpart. Second, internal conversion necessitates a coupling between electronic states mediated by a change in the nuclear structure of each state along a participating vibrational coordinate, as captured by the quantity C. For large changes in structure, states couple more strongly together via the Franck−Condon mechanism and the nonradiative relaxation process needs a smaller value of C to occur. For smaller changes in nuclear structure, the Franck−Condon factors are smaller and a larger value of C is needed to induce nonradiative relaxation. Despite the known importance of the dependence of the internal conversion decay rate on these characteristics of the involved electronic states, their interdependence with the energy gap and their inaccurate prediction via ab initio methods inhibit the use of eq 2 as a guide for controlling internal conversion decay rates via traditional synthetic methods.

Because we seek to establish a fundamental physical understanding of how the quantum fluctuations of cavity-confined photons affect ultrafast nonradiative relaxation, we modeled the internal conversion decay rates as a function of the energy gap between the S_1 state of ZnTPP and either the S_2 or the lower polariton states, depending on the specific sample, as described in eq 2. In this model, we presume the vibration of interest is a ring distortion possessing an effective frequency of 1190 cm^{-1} ($\hbar\omega_\nu$ = 0.1475 eV), given the separation of the peaks in the linear absorption spectrum shown in the left panel of Figure 1 and established previously.[34] We also presume the energy of the S_1 state remains the same relative to the molecule's ground state as we change the collective vacuum Rabi splitting energy. Figure 5 shows the results of this modeling. We find the decay rate of each of our samples does not match the expected trend based on eq 2. In particular, we extract values of 2.573 eV and 0.0881 for C and Δ_ν, respectively. Analysis of the ultraviolet−visible absorption spectrum of ZnTPP suggests S_2 possesses a Δ_ν of 0.1538 relative to S_0. Given many authors conclude the S_0 and S_1 states possess the same equilibrium structure, this displacement would also refer to that of S_2 relative to S_1, which is a factor of 2 larger than the value found from modeling the internal conversion rates with eq 2. When we consider the possibility that internal conversion occurs via C−H stretching vibrations at 3300 cm^{-1} (0.41 eV), the values extracted from our model change to C = 6.724 eV and Δ_ν = 0.0003157 with no significant improvement in the resulting fit to the measured data, as shown in Figure S4.

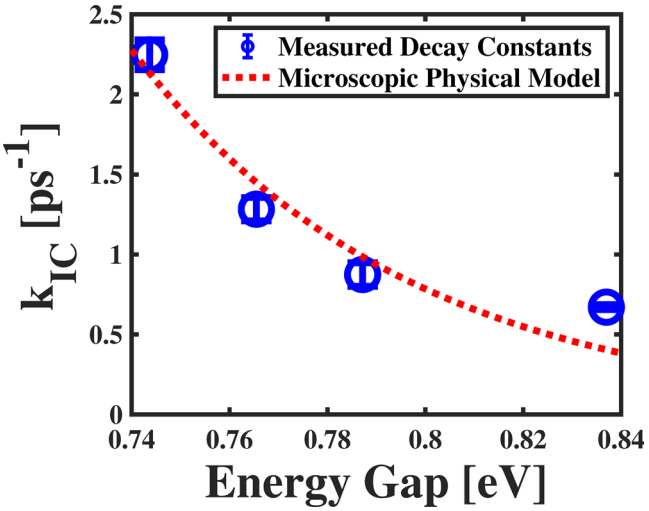

Figure 5. Comparison of the trend in measured internal conversion decay rates for solution phase and strongly cavity-coupled ZnTPP molecules to a microscopic model developed by Jortner and co-workers, as described explicitly by eq 2.

The results of our analysis shown in Figure 5 suggest some physical parameter of cavity polariton formation besides the energy gap between the participating electronic states affects the internal conversion rate. Two facets of the effect of cavity polariton formation emerge as possible explanations for the deficiency of the standard theory based solely on energy gaps. First, it is possible the formation of cavity polaritons changes not only the energies of the polariton states themselves but also the energies of closely lying electronic states of the strongly coupled molecules. To test this idea, we measured the steady state fluorescence emitted by the S_1 state following excitation at 2.33 eV (532 nm), as shown in Figure S5. Given the lack of any significant shifts in the peak positions of these spectra, our tests suggest cavity polariton formation does not affect the energy of the S_1 state relative to that of the ground state, S_0. Therefore, even though we systematically push the energy of the lower polariton state closer and closer to that of the S_1 state, there does not seem to be evidence that the S_1 energy changes as a function of the collective vacuum Rabi splitting.

Second, a fundamental interpretation of physical parameters in eq 2 suggests any changes in the equilibrium structure of a molecule induced by polariton formation could play a significant role in the observed dynamics. Specifically, the direct dependence of the internal conversion rate on the dimensionless displacement, Δ_ν, could be a route to polaritonic control of molecular dynamics based on the results of previous theoretical studies.[13−18] To assess this idea, we phenomenologically investigated changes to Δ_ν of a single, harmonic mode induced by polariton formation within a framework proposed by Mukamel and co-workers[17] that we previously extended to polyatomic molecules.[34] We use this model to calculate how the S_2 potential energy surface changes upon polariton formation and how these changes affect the Δ_ν of the lower polariton relative to the unaffected S_1 state.

Briefly, we construct these potential energy surfaces from a force constant and reduced mass for a totally symmetric vibration near 1190 cm^{-1} determined by density functional theory calculations, as reported in our previous study.[34] We then use these potential energy surfaces to diagonalize a

https://dx.doi.org/10.1021/acs.jpclett.9b03447
J. Phys. Chem. Lett. 2020, 11, 1013−1021

harmonic oscillator Hamiltonian for each of the pertinent electronic states numerically to produce their respective vibrational frequencies and minima as a function of the vibrational coordinate. For the case of a free space molecule, these electronic states would include S_0−S_2 of the ZnTPP molecule, while we would introduce the polariton potential energy surfaces in place of that of the S_2 state for the case of strong light−molecule coupling. With the vibrational parameters of each surface, we can numerically establish how the dimensionless displacement changes upon polariton formation and for different polariton parameters. As shown in Figure 6,

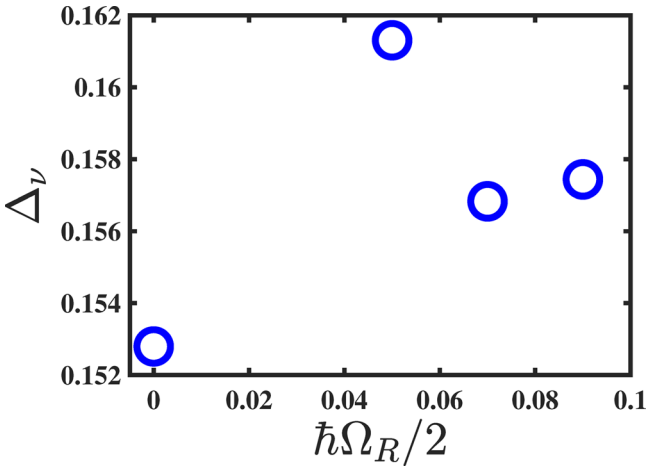

Figure 6. Numerically calculated dependence of the dimensionless displacement of the lower polaritonic potential energy surface relative to the S_1 state of zinc(II) tetraphenylporphyrin found as a function of the collective vacuum Rabi splitting energy, $\hbar\Omega_R$. The trend found from these numerical calculations does not account for the discrepancies between our measured polaritonic internal conversion decay rates and the rates predicted by standard microscopic physical theories.

this simple model does not predict a trend in Δ_ν for different collective vacuum Rabi splitting values consistent with the measured internal conversion rate constants. In particular, while our results indicate the internal conversion rates for $\hbar\Omega$/2 values of 0.05 and 0.07 eV fall below the predictions of Jortner's model, the Δ_ν values we find from our phenomenological model at similar collective vacuum Rabi splitting values should coincide with increases in the internal conversion rate. On the basis of this disagreement, we tentatively conclude structural changes like those predicted by proposed theories cannot adequately explain our experimental results. More advanced structural models of polariton formation must be developed.

Given the inability of the Jortner model to explain the changes in the internal conversion rate as a function of the collective vacuum Rabi splitting energy, we explore other possible explanations of the trend shown in Figure 5. In particular, we propose the formation of polaritons introduces an additional channel through which the excited molecules can relax into the S_1 state. For this type of model, we assume the total internal conversion rate is the sum of two terms: one term due to relaxation of the free space molecules and another due to polariton formation using a test function of the collective vacuum Rabi splitting

$$k_{IC} = k_{IC}^{cp}\left(\frac{\hbar\Omega}{2E_0}\right)^P + k_{IC}^0 \tag{3}$$

where k_{IC}^0 is the internal conversion rate of the free space molecules, which is determined from the nonlinear regression analysis of the solution phase ultrafast transient absorption detailed in the Supporting Information, k_{IC}^{cp} is the rate of polariton-induced internal conversion, and E_0 and P parametrize this additional decay channel. Figure 7 compares the

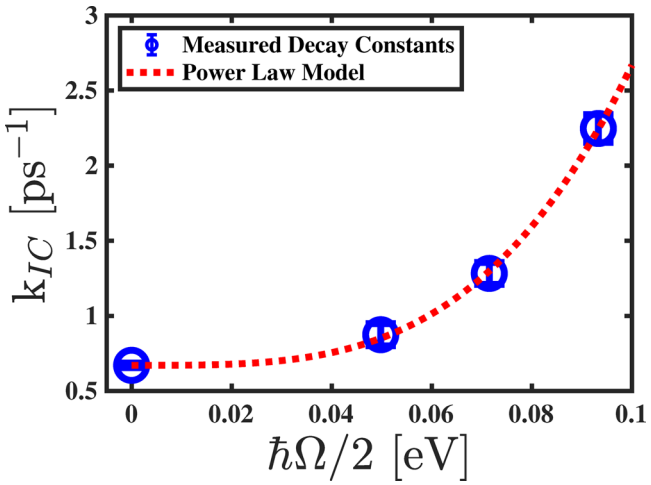

Figure 7. Comparison of the trend in measured internal conversion decay rates for solution phase and strongly cavity-coupled ZnTPP molecules to a power law fit using eq 3.

results of modeling the observed internal conversion rates using eq 3 to the measured internal conversion rates with their uncertainties shown as error bars. Through this analysis, we find the following model values: k_{IC}^{cp} = 0.3018 ps^{-1}, E_0 = 0.05781 eV, and P = 3.449.

In conclusion, we have demonstrated controlling concentrations of ZnTPP within electromagnetic resonator structures can be used to directly control the ultrafast internal conversion dynamics of molecules strongly coupled to the cavity's virtual photons. Moreover, we showed this control depends on the energy gap between the lower cavity polariton and the S_1 state of ZnTPP. The changes in the measured ultrafast dynamics of the polaritons we form point to microscopic physics beyond the models typically used to explain nonradiative relaxation. In particular, the phenomenological model proposed by Englman and Jortner cannot adequately explain the trend in internal conversion as a function of the energy gap between the delocalized polaritonic states and localized molecular states. Furthermore, a simple, single-mode model like those used to predict how the structure of molecules changes in the presence of strong cavity coupling does not produce trends in the pertinent parameters of the Englman−Jortner model consistent with its deviations from our experimental results. This inability to explain the difference between the measured ultrafast dynamics and the predictions of a standard model suggests one must take great care in attempting to predict how the structure of complex, polyatomic molecules will change in response to cavity polariton formation.

Given the prominence of nonadiabatic coupling mechanisms in the photophysics of metalloporphyrins, a specialized model appropriately accounting for frequency shifts and non-Condon vibronic coupling effects may be necessary to explain our

https://dx.doi.org/10.1021/acs.jpclett.9b03447
J. Phys. Chem. Lett. 2020, 11, 1013−1021

results. These effects may emerge from more advanced ultrafast spectroscopic experimental techniques in which one coherently modulates the structure of cavity-embedded molecules to directly assess how polaritonic PESs change relative to their free space counterparts.[35−38] However, such a development is beyond the scope of this study.

While the Englman−Jortner model of the decay constants cannot account for the observed trend in the nonradiative relaxation between the LP and S_1 states of the strongly coupled ZnTPP molecules, the good agreement between the modeled and measured internal conversion rates shown in Figure 7 suggests polariton formation introduces nonradiative relaxation channels unavailable to molecules not strongly coupled to the virtual photons of an electromagnetic cavity. In addition, once polariton formation introduces these channels, the rate at which they cause nonradiative relaxation seems to add to the rate caused by the internal structure of the free space molecule. Furthermore, the values we extract from fitting our measured internal conversion rates to the model in eq 3 motivate us to speculate about some of the microscopic physics occurring during the measurements. Specifically, the energy E_0 falls within the range of low-frequency ring distortions of the porphyrin molecule and could signify its participation in the nonradiative transition between the polaritonic and non-polaritonic manifolds of the light−molecule system. More studies comparing the vibrational spectra and polariton-amended internal conversion dynamics will be needed to assess this hypothesis.

Our results indicate the ultrafast photophysics of metalloporphyrins can be controlled using cavity polariton formation, and this mechanism provides precision in controlling the rates of nonradiative relaxation. On the basis of our straightforward approach detailed above, this control can be applied to enhance porphyrin moieties in nanomaterials for photocatalytic and optoelectronic applications. For example, cavity polariton formation using metalloporphyrin arrays could lead to deterministic control over the initial pathways to electron transfer and subsequent photocatalytic activity, as pioneered by Holten et al.[7]

In addition to enabling control over the capabilities of porphyrin molecular moieties in materials science, cavity polariton formation can be used to disentangle the ultrafast mechanisms of energy transfer and charge separation in biologically relevant systems containing porphyrin or porphyrin-like molecular constituents such as light-harvesting proteins. We envision fabricating cavity structures similar to those we have studied here in which these biological systems are embedded with differing concentrations. The modulation of electronic energy gaps via control over the collective vacuum Rabi splitting could serve as a deterministic method to control and decipher the electronic states involved in nonradiative processes in addition to methods like molecular mutations at specific sites.[39] With an additional handle capable of controlling the electronic structure of the light-activated molecules, our results show researchers can use control over the collective vacuum Rabi splitting of cavity polariton states to enable better performance of porphyrin materials and a better understanding of porphyrins in biology.

METHODS

Zinc(II) tetraphenyl porphyrin (ZnTPP) was purchased from Sigma-Aldrich and used without further purification. Thin films of poly-methyl methacrylate (PMMA) were formed by spinning a commercially available solution containing the polymer (MicroChem) on the substrate of choice using a commercial spin coater (Laurell WS-650Mz-23NPPB) followed by annealing the resulting substrate/film system at 180 °C for 3 min to cure the film. ZnTPP was added to the polymer solution prior to the spin coating process to appropriately dope the resulting film. To charactarize the doped film linear absorption measurements, we made a 0.959 mM ZnTPP concentration PMMA solution and spun it on a clean microscope slide at 1900 rpm. The ultraviolet−visible absorption spectrum was then acquired with a Jasco-V-570 spectrophotometer.

Cavity polariton samples were formed by fabricating a custom-designed distributed Bragg reflector (DBR) from alternating layers of SiO_2 and Si_3N_4 on cleaned, optical grade fused silica substrates using chemical vapor deposition. The stop band of the DBR structures was chosen to overlap with the Soret resonance of the ZnTPP, as established from ultraviolet−visible absorption measurements shown in Figure S1. We then spun samples of 1.989, 0.988, and 0.494 mM ZnTPP concentration PMMA solutions at 5500 rpm on top of the DBR structure. Ellipsometry measurements show we form ∼140 nm films with these spin processing parameters. Following curing of the doped polymer film, we deposited ∼15 nm films of Al over the films to form the Fabry−Perot resonators. We checked for the successful formation of cavity polaritons using angle-resolved transmission measurements. The beam from a commercial halogen lamp (Thorlabs QTH10) was focused through the cavity structure at different incident angles, collected, and then detected in a fiber-coupled dispersive spectrometer (OceanOptics OceanFX).

Ultrafast transient reflectivity measurements were carried out using the 1.55 eV output of a regenerative amplified seed pulse from a titanium-doped sapphire oscillator (Spectra Physics Solstice Ace). Part of the output was used to pump a frequency convertor to generate 3.1 eV pump pulses. Another part of the laser output was passed through a delay stage assembly, spatially filtered, and focused into a 3 mm thick sapphire plate to generate the white light continuum. The white light continuum was then passed through a short pass filter with a 90% transmission edge at 1.65 eV (Thorlabs FESH0750) to reject residual intensity at 1.55 eV. The two beams were then steered to the sample and overlapped in space using a pinhole. The portion of the probe beam reflected from the sample was then steered to a Si photodiode affixed with a 30 meV wide bandpass filter centered at 1.97 eV. We angled the substrate surface to put the ZnTPP Soret transition and cavity mode in resonance when considering the pump incidence direction.

ASSOCIATED CONTENT

Supporting Information

The Supporting Information is available free of charge at https://pubs.acs.org/doi/10.1021/acs.jpclett.9b03447.

DBR transmission spectra, comparisons of the polariton spectra for cavities possessing different concentrations of ZnTPP, an ultrafast transient absorption kinetic trace of solvated ZnTPP, the full set of parameters extracted from fitting measured kinetic traces to the physical models described in the text, a comparison of the fitting of extracted internal conversion rates for different types of participating vibrations, and fluorescence spectra

https://dx.doi.org/10.1021/acs.jpclett.9b03447
J. Phys. Chem. Lett. 2020, 11, 1013−1021

emitted by the S_1 state of ZnTPP in different polymer environments (PDF)

AUTHOR INFORMATION

Corresponding Author

Aaron S. Rury − *Department of Chemistry, Wayne State University, Detroit, Michigan 48202, United States;* orcid.org/0000-0002-1836-1424; Email: aaron.rury@wayne.edu

Author

Aleksandr G. Avramenko − *Department of Chemistry, Wayne State University, Detroit, Michigan 48202, United States*

Complete contact information is available at: https://pubs.acs.org/10.1021/acs.jpclett.9b03447

Notes

The authors declare no competing financial interest.

ACKNOWLEDGMENTS

The work reported here was supported by the Air Force Office of Scientific Research through its Young Investigator Program by Grant FA9550-19-1-0231 and the American Chemical Society Petroleum Research Fund through Grant 60003-DNI6. The Fabry−Perot cavity structures used to form cavity polaritons were fabricated at the Lurie Nanofabrication Facility of the University of Michigan (Ann Arbor, MI). The authors thank Dr. Thomas Knisley for his assistance with ellipsometric measurements used to establish the thickness of doped and undoped PMMA films.

REFERENCES

(1) Kober, E. M.; Caspar, J. V.; Lumpkin, R. S.; Meyer, T. J. Application of the Energy Gap Law to Excited-State Decay of Osmium(II)-polypyridine Complexes: Calculation of Relative Nonradiative Decay Rates from Emission Spectral Profiles. *J. Phys. Chem.* **1986**, *90*, 3722−3734.

(2) Cummings, S. D.; Eisenberg, R. Tuning the Excited-State Properties of Platinum(II) Diimine Dithiolate Complexes. *J. Am. Chem. Soc.* **1996**, *118*, 1949−1960.

(3) Li, J.; Djurovich, P. I.; Alleyne, B. D.; Yousufuddin, M.; Ho, N. N.; Thomas, J. C.; Peters, J. C.; Bau, R.; Thompson, M. E. Synthetic Control of Excited-State Properties in Cyclometalated Ir(III) Complexes Using Ancillary Ligands. *Inorg. Chem.* **2005**, *44*, 1713−1727.

(4) Ebbesen, T. W. Hybrid Light-Matter States in a Molecular and Material Science Perspective. *Acc. Chem. Res.* **2016**, *49*, 2403−2412.

(5) Lidzey, D. G.; Bradley, D. D. C.; Skolnick, M. S.; Virgili, T.; Walker, S.; Whittaker, D. M. Strong Exciton-Photon Coupling in an Organic Semiconductor Microcavity. *Nature* **1998**, *395*, 53−55.

(6) Li, F.; Yang, S. I.; Ciringh, Y.; Seth, J.; Martin, C. H.; Singh, D. L.; Kim, D.; Birge, R. R.; Bocian, D. F.; Holten, D.; et al. Design, Synthesis, and Photodynamics of Light-Harvesting Arrays Comprised of a Porphyrin and One, Two, or Eight Boron-Dipyrrin Accessory Pigments. *J. Am. Chem. Soc.* **1998**, *120*, 10001−10017.

(7) Holten, D.; Bocian, D. F.; Lindsey, J. S. Probing Electronic Communication in Covalently Linked Multiporphyrin Arrays. A Guide to the Rational Design of Molecular Photonic Devices. *Acc. Chem. Res.* **2002**, *35*, 57−69.

(8) Kim, D.; Osuka, A. Photophysical Properties of Directly Linked Linear Porphyrin Arrays. *J. Phys. Chem. A* **2003**, *107*, 8791−8816.

(9) Kodis, G.; Liddell, P. A.; de la Garza, L.; Clausen, P. C.; Lindsey, J. S.; Moore, A. L.; Moore, T. A.; Gust, D. Efficient Energy Transfer and Electron Transfer in an Artificial Photosynthetic Antenna-Reaction Center Complex. *J. Phys. Chem. A* **2002**, *106*, 2036−2048.

(10) Wasielewski, M. R. Photoinduced Electron Transfer in Supramolecular Systems for Artificial Photosynthesis. *Chem. Rev.* **1992**, *92*, 435−461.

(11) Kuciauskas, D.; Liddell, P. A.; Lin, S.; Johnson, T. E.; Weghorn, S. J.; Lindsey, J. S.; Moore, A. L.; Moore, T. A.; Gust, D. An Artificial Photosynthetic Antenna-Reaction Center Complex. *J. Am. Chem. Soc.* **1999**, *121*, 8604−8614.

(12) Savolainen, J.; Fanciulli, R.; Dijkhuizen, N.; Moore, A. L.; Hauer, J.; Buckup, T.; Motzkus, M.; Herek, J. L. Controlling the Efficiency of an Artificial Light-Harvesting Complex. *Proc. Natl. Acad. Sci. U. S. A.* **2008**, *105*, 7641−7646.

(13) Galego, J.; Garcia-Vidal, F. J.; Feist, J. Cavity-Induced Modifications of Molecular Structure in the Strong-Coupling Regime. *Phys. Rev. X* **2015**, *5*, 041022.

(14) Spano, F. C. Optical Microcavities Enhance the Exciton Coherence Length and Eliminate Vibronic Coupling in J-aggregates. *J. Chem. Phys.* **2015**, *142*, 184707.

(15) Herrera, F.; Spano, F. C. Cavity-Controlled Chemistry in Molecular Ensembles. *Phys. Rev. Lett.* **2016**, *116*, 238301.

(16) Kowalewski, M.; Bennett, K.; Mukamel, S. Cavity Femtochemistry: Manipulating Nonadiabatic Dynamics at Avoided Crossings. *J. Phys. Chem. Lett.* **2016**, *7*, 2050−2054.

(17) Kowalewski, M.; Bennett, K.; Mukamel, S. Non-adiabatic Dynamics of Molecules in Optical Cavities. *J. Chem. Phys.* **2016**, *144*, 054309.

(18) Flick, J.; Ruggenthaler, M.; Appel, H.; Rubio, A. Atoms and Molecules in Cavities, from Weak to Strong Coupling in Quantum-Electrodynamics (QED) Chemistry. *Proc. Natl. Acad. Sci. U. S. A.* **2017**, *114*, 3026−3034.

(19) Yu, H.-Z.; Baskin, J. S.; Zewail, A. H. Ultrafast Dynamics of Porphyrins in the Condensed Phase: II. Zinc Tetraphenylporphyrin. *J. Phys. Chem. A* **2002**, *106*, 9845−9854.

(20) Lidzey, D. G.; Fox, A. M.; Rahn, M. D.; Skolnick, M. S.; Agranovich, V. M.; Walker, S. Experimental Study of Light Emission from Strongly Coupled Organic Semiconductor Microcavities following Nonresonant Laser Excitation. *Phys. Rev. B: Condens. Matter Mater. Phys.* **2002**, *65*, 195312.

(21) Coles, D. M.; Michetti, P.; Clark, C.; Tsoi, W. C.; Adawi, A. M.; Kim, J.-S.; Lidzey, D. G. Vibrationally Assisted Polariton-Relaxation Processes in Strongly Coupled Organic-Semiconductor Microcavities. *Adv. Funct. Mater.* **2011**, *21*, 3691−3696.

(22) Savvidis, P. G.; Connolly, L. G.; Skolnick, M. S.; Lidzey, D. G.; Baumberg, J. J. Ultrafast Polariton Dynamics in Strongly Coupled Zinc Porphyrin Microcavities at Room Temperature. *Phys. Rev. B: Condens. Matter Mater. Phys.* **2006**, *74*, 113312.

(23) Tas, G.; Maris, H. J. Electron Diffusion in Metals Studied by Picosecond Ultrasonics. *Phys. Rev. B: Condens. Matter Mater. Phys.* **1994**, *49*, 15046−15054.

(24) Nisoli, M.; De Silvestri, S.; Cavalleri, A.; Malvezzi, A. M.; Stella, A.; Lanzani, G.; Cheyssac, P.; Kofman, R. Coherent Acoustic Oscillations in Metallic Nanoparticles Generated with Femtosecond Optical Pulses. *Phys. Rev. B: Condens. Matter Mater. Phys.* **1997**, *55*, R13424−R13427.

(25) Perner, M.; Gresillon, S.; März, J.; von Plessen, G.; Feldmann, J.; Porstendorfer, J.; Berg, K.-J.; Berg, G. Observation of Hot-Electron Pressure in the Vibration Dynamics of Metal Nanoparticles. *Phys. Rev. Lett.* **2000**, *85*, 792−795.

(26) Park, H.; Wang, X.; Nie, S.; Clinite, R.; Cao, J. Mechanism of Coherent Acoustic Phonon Generation Under Nonequilibrium Conditions. *Phys. Rev. B: Condens. Matter Mater. Phys.* **2005**, *72*, 100301.

(27) Virgili, T.; Coles, D.; Adawi, A. M.; Clark, C.; Michetti, P.; Rajendran, S. K.; Brida, D.; Polli, D.; Cerullo, G.; Lidzey, D. G. Ultrafast Polariton Relaxation Dynamics in an Organic Semiconductor Microcavity. *Phys. Rev. B: Condens. Matter Mater. Phys.* **2011**, *83*, 245309.

(28) Robinson, G. W.; Frosch, R. P. Electronic Excitation Transfer and Relaxation. *J. Chem. Phys.* **1963**, *38*, 1187−1203.

(29) Siebrand, W. Radiationless Transitions in Polyatomic Molecules. I. Calculation of Franck—Condon Factors. *J. Chem. Phys.* **1967**, *46*, 440−447.
(30) Siebrand, W. Radiationless Transitions in Polyatomic Molecules. II. Triplet-Ground-State Transitions in Aromatic Hydrocarbons. *J. Chem. Phys.* **1967**, *47*, 2411−2422.
(31) Bixon, M.; Jortner, J. Intramolecular Radiationless Transitions. *J. Chem. Phys.* **1968**, *48*, 715−726.
(32) Englman, R.; Jortner, J. The Energy Gap Law for Radiationless Transitions in Large Molecules. *Mol. Phys.* **1970**, *18*, 145−164.
(33) Freed, K. F.; Jortner, J. Multiphonon Processes in the Nonradiative Decay of Large Molecules. *J. Chem. Phys.* **1970**, *52*, 6272−6291.
(34) Avramenko, A. G.; Rury, A. S. Interrogating the Structure of Molecular Cavity Polaritons with Resonance Raman Scattering: An Experimentally Motivated Theoretical Description. *J. Phys. Chem. C* **2019**, *123*, 30551−30561.
(35) Kano, H.; Saito, T.; Kobayashi, T. Observation of Herzberg-Teller-type Wave Packet Motion in Porphyrin J-Aggregates Studied by Sub-5-fs Spectroscopy. *J. Phys. Chem. A* **2002**, *106*, 3445−3453.
(36) Rury, A. S.; Sorenson, S.; Driscoll, E.; Dawlaty, J. M. Electronic State-Resolved Electron-Phonon Coupling in an Organic Charge Transfer Material from Broadband Quantum Beat Spectroscopy. *J. Phys. Chem. Lett.* **2015**, *6*, 3560−3564.
(37) Rury, A. S.; Sorenson, S. A.; Dawlaty, J. M. Coherent Vibrational Probes of Hydrogen Bond Structure Following Ultrafast Electron Transfer. *J. Phys. Chem. C* **2016**, *120*, 21740−21750.
(38) Rury, A. S.; Sorenson, S. A.; Dawlaty, J. M. Evidence of Ultrafast Charge Transfer Driven by Coherent Lattice Vibrations. *J. Phys. Chem. Lett.* **2017**, *8*, 181−187.
(39) Maiuri, M.; Ostroumov, E. E.; Saer, R. G.; Blankenship, R. E.; Scholes, G. D. Coherent Wavepackets in the Fenna−Matthews−Olson Complex are Robust to Excitonic-structure Perturbations caused by mutagenesis. *Nat. Chem.* **2018**, *10*, 177−183.

https://dx.doi.org/10.1021/acs.jpclett.9b03447
J. Phys. Chem. Lett. 2020, 11, 1013−1021